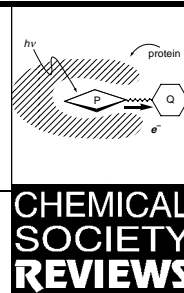


Molecular modelling of electron transfer systems by noncovalently linked porphyrin–acceptor pairing



CHEMICAL
SOCIETY
REVIEWS

Takashi Hayashi† and Hisanobu Ogoshi†

Department of Synthetic Chemistry and Biological Chemistry, Graduate School of Engineering, Kyoto University, Kyoto 606-01, Japan

In the respiratory system, electron carriers such as ubiquinone and cytochrome c play an important role in the electron transfer (ET) reaction between oxidoreductases embedded in the mitochondrial membrane. This review focuses on a strategy for constructing porphyrin–electron acceptor pairs *via* specific interactions and the evaluation of ET in these systems. Particularly, the molecular recognition of ubiquinone analogues by porphyrin host molecules and the mimicking of protein–protein complexation using myoglobin reconstituted with a synthetic porphyrin are reviewed, and the characteristics of the photoinduced ET within noncovalently linked complexes are discussed.

1 General introduction

Electron transfer (ET) reactions in biological systems provide one of the most fascinating fields of current interdisciplinary research. It is well known that ET occurring within mitochondria and chloroplasts plays a crucial role in respiratory oxidative phosphorylation and photosynthesis, in which many oxidoreductases are embedded in the membrane and moveable electron carriers are organized. These two systems produce the high energy ATP through multi ET reactions and proton flux by action of the membrane-bound enzymes. Therefore, it is of particular interest for chemists and biochemists to elucidate the ET systems, both experimentally and theoretically.

Although, in general, the natural system is quite complicated, we know that simple synthetic models focusing on the function

of the target enzyme often give us good information with regard to the reaction mechanisms and/or some structural features of important components. Over the last decade, biomimetic model systems have been suitable for the discussion of the ET mechanism. After elucidation of the crystal structure of the bacterial photosynthetic reaction centre,¹ a great number of covalently linked donor–spacer–acceptor models have been reported in the literature, some of them giving valuable insight into the ET mechanism through focusing on donor–acceptor distances and their relative special organization, features of the spacer, driving force, and solvent effect. In particular, models based on covalently linked donor–acceptor systems such as porphyrin–spacer–porphyrin or porphyrin–spacer–quinone suggest that the unique organization of the characteristic chromophores found in the photochemical reaction centre is responsible for the highly efficient charge separation.^{2,3} In contrast, noncovalently linked donor–acceptor complexes are essential models towards the understanding of the ET reaction in the respiratory system, in which electron transport is accomplished by specific mobile carriers such as ubiquinone and cytochrome c. However, studies on noncovalently linked donor–acceptor systems with specific interactions *via* molecular recognition remain quite limited.⁴ Thus, this has stimulated the design of new donor–acceptor complexes based on weak noncovalent interactions such as hydrogen bonds, salt bridges and van der Waals contacts and the subsequent investigation of the long-range ET reaction.

2 The respiratory system in the mitochondrial membrane

Fig. 1 shows the schematic pathway of ET from NADH to O₂ in the respiratory mitochondrial membrane, where two electron carriers control the overall rate of ET process *via* specific interaction with the membrane-bound oxidoreductases. Ubiqui-

† Present addresses: T. H., Department of Chemistry and Biochemistry, Graduate School of Engineering, Kyushu University, Higashi-ku, Fukuoka 812-81, Japan; H.O., Fukui National College of Technology, Geshi, Sabae 916, Japan.

Takashi Hayashi was born in 1962 in Osaka. He received his PhD at Kyoto University working under the supervision of Y. Ito. He was then an assistant professor (1990–1997) at Kyoto



Takashi Hayashi

University. In July of 1997 he moved to Kyushu University as an associate professor. He stayed at I. Bertini's laboratory at University of Florence (Italy) in 1986. From 1995 to 1996, he was working with C.-H. Wong at the Scripps Research Institute (USA) as a visiting researcher. His current interests are bioorganic and bioorganic chemistry, particularly, molecular recognition and porphyrin chemistry.

Hisanobu Ogoshi was born in 1934. He received his education from Kyoto University. In 1963–1965, he was a research associate of Illinois Institute of Technology (USA). After that, he



Hisanobu Ogoshi

joined the staff of Department of Synthetic Chemistry at Kyoto University. He moved to Nagasaki Institute of Technology as a full professor in 1980 and returned to Kyoto University in 1988. He organized the Seventh International Symposium on Molecular Recognition and Inclusion at Kyoto in 1992. In April of 1997, he moved to the Fukui National College of Technology as a president and became an emeritus professor of Kyoto University.

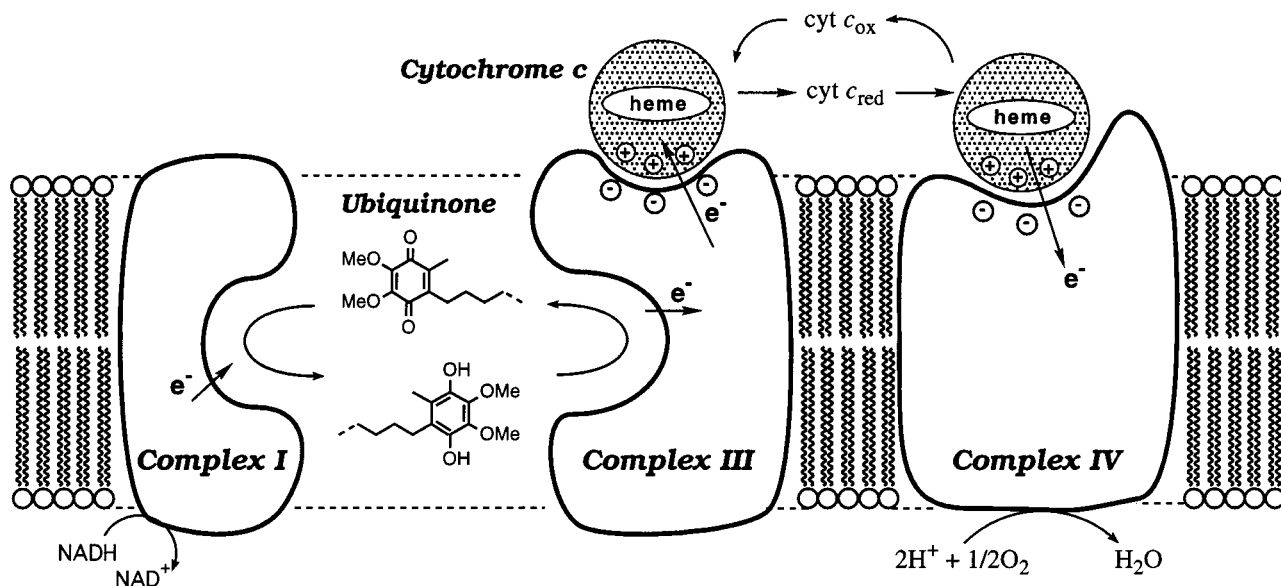


Fig. 1 A schematic diagram of the mitochondrial electron transport chain indicating the ET pathway. Complex II is not shown. The shape of each complex is simplified and different from the real structure in order to emphasize the interaction sites for electron carriers. Proton flux through the membrane is omitted.

none has two methoxy groups at the 2- and 3-positions on the quinone ring and a long hydrophobic isoprenoid chain which makes it soluble in the inner mitochondrial membrane lipid bilayer. It was thought that electrons are smoothly shuttled from NADH-coenzyme Q reductase (Complex I) to ubiquinone and from reduced ubiquinone, ubiquinol, to Coenzyme Q-cytochrome c reductase (Complex III) via specific binding sites in each complex, although no X-ray structure has ever been solved with satisfactory resolution. Enzyme studies using synthetic ubiquinone or ubiquinol analogues have provided us with helpful information about the specific binding sites for electron carrier in the huge Complex I or Complex III, suggesting the importance of structural features of quinone substituents (alkyl and alkoxy groups) upon binding with proteins.⁵

Cytochrome c is another important electron carrier between Complex III and cytochrome c oxidase (Complex IV). This haemoprotein, one of the well-known cytochromes, is almost spherical and contains 104 amino acid residues. One of the significant features regarding the structure of cytochrome c is that several lysines are distributed on the surface of the protein near the haem concave. In fact, according to the X-ray study of cytochrome c–cytochrome c peroxidase (CCP) complex, positive residues of cytochrome c, Lys73 and Lys87, form special ion pairs with negative residues of CCP, Glu290 and Asp34, respectively.⁶ In the respiratory system, it is known that Complexes III and IV have binding sites including acidic residues for highly basic cytochrome c. Furthermore, the high resolution X-ray structures of Complex IV from *Paracoccus denitrificans* and bovine heart have recently been reported.⁷ According to these analyses, the binding site of Complex IV contains several acidic residues which could interact with lysine residues on the surface of cytochrome c.

3 Model studies on noncovalently linked donor–acceptor complexes

In nature, organization is quite often the result of supramolecular assembly based on noncovalent intermolecular interactions via specific molecular recognition of protein–protein, protein–sugar, DNA–receptor, antigen–antibody *etc.* Thereby host–guest chemistry and supramolecular chemistry based on molecular recognition processes have grown very rapidly along the elucidation of biological systems. In the case of ET systems aimed at mimicking complex natural processes, the design of

donor–acceptor assemblies based on weak intermolecular interactions (for example, hydrogen bonding, salt bridge, and/or van der Waals contact) has been regarded as a suitable approach.

We and several other groups have focused on the respiratory system, particularly, ET via electron carriers for a few years, and begun to construct the ET model using noncovalently linked donor–acceptor systems. Currently, our research can be divided into two approaches: preparation of a new ubiquinone receptor based on a functional porphyrin and investigation of its molecular recognition behaviour and mimicking of protein–protein complexation using a reconstituted myoglobin whose surface shows a specific binding interface. In this review, we wish to describe the strategy of molecular recognition for electron carriers and the ET reaction between photoexcited porphyrin and electron carriers.

4 Porphyrin–ubiquinone analogue complex via hydrogen bonding

To our knowledge, examples of noncovalently linked porphyrin–quinone pairs aimed at ET model systems are very few. In 1990, Ogoshi and co-workers have reported the cofacial interaction of functional porphyrin, 5,15-*cis*-bis(2-hydroxy-1-naphthyl)octaethylporphyrin (**2**) and several quinones by use of two-point hydrogen bonds between carbonyl oxygen of quinone and phenolic protons of porphyrin.⁸ Sessler and co-workers have presented a sideways-linked porphyrin–quinone complex via base pairing and demonstrated the photoinduced ET reaction.⁹

The previous porphyrin host molecules,^{8,9,10} however, are limited to quinone guests, since almost all host molecules can only bind *p*-benzoquinone or duroquinone analogues. Furthermore, although the ET studies in the porphyrin–quinone pairings showed the quinone quenching properties and allowed estimation of the forward ET rate through fluorescence lifetime measurements, there has been no direct evidence of any separated-charge state as a product of ET reaction, except in one report.^{9c} Recently, we have prepared a new host porphyrin for ubiquinone, the latter being an important electron carrier in the respiratory system.¹¹ In the following sections, we briefly present the specific interactions between this functional porphyrin and some ubiquinone analogues as well as the ET reaction occurring within this noncovalently linked complex.

4.1 Molecular recognition of ubiquinone analogues

When we design a host molecule for a target guest, the following factors seem to be important: (i) preorganization of the host providing sufficient affinity with the guest molecule structure and (ii) the multifunctionalization of the host molecule to increase the specificity of host–guest complex. Considering these two factors, the porphyrin ring is an attractive potential host molecule, its relatively flat and rigid structure being suitable as a receptor framework and allowing easy introduction of various functional groups.¹² Furthermore, porphyrin has unique photoreactivity characteristics and redox behaviour, thus we adopted it as a host molecule for ubiquinone analogues. Although the structure of the ubiquinone binding site is not known with accuracy, we have postulated that several protein residues such as tyrosine interact with ubiquinone through hydrogen bonds with phenolic protons. Consequently, we have prepared the *meso*- $\alpha,\alpha,\alpha,\alpha$ -tetra(2-hydroxy-1-naphthyl)-porphyrin (**1**) as a host molecule.^{11a}

Host **1** was obtained from the condensation of pyrrole and 2-methoxy-1-naphthylaldehyde and the following deprotection of methyl groups in sufficient yield. The obtained atropisomeric mixture was easily separated by classical silica gel chromatography and the atropisomerization derived from internal rotation about C(*meso*)-C(*ipso*) bonds was not observed even in boiling toluene. The interaction between **1** and quinone was monitored by NMR, IR and UV–VIS spectroscopic measurements, which show the cofacial 1 : 1 complex in chloroform and toluene. The summary of spectroscopic features is shown in Fig. 2. The OH proton signal of **1** was shifted downfield by 1.91 ppm and the OH stretching frequency of **1** was replaced by a new absorption at 3449 cm⁻¹ in the presence of 1 equiv. of tetramethoxy-*p*-benzoquinone (**4c**), which indicates that the four OH groups of **1** enter hydrogen bonding interaction with **4c**. The upfield shift of methoxy protons of **4c** is due to the porphyrin ring

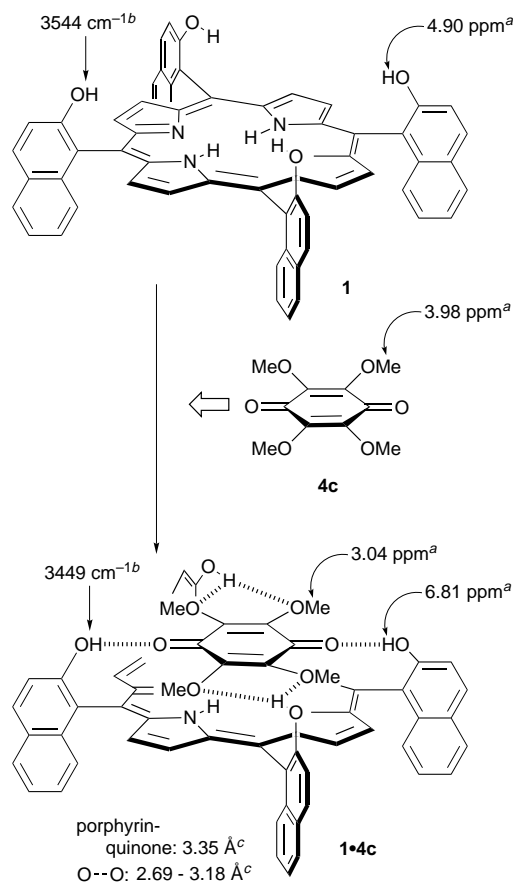


Fig. 2 Structural data of **1** and **1·4c**. (a) ¹H NMR chemical shifts in CDCl₃. (b) IR data of OH stretching in CHCl₃. (c) X-Ray crystal structure analysis.

current. X-Ray crystal structure analysis shows the cofacial porphyrin–quinone assembly with a cofacial distance of 3.35 Å.^{11c}

Binding constants were determined from UV–VIS spectrophotometric titration of various quinones with CHCl₃ solution of **1**, using the spectral change from 550 to 700 nm with several isosbestic points (Fig. 3). Selected binding constants and their

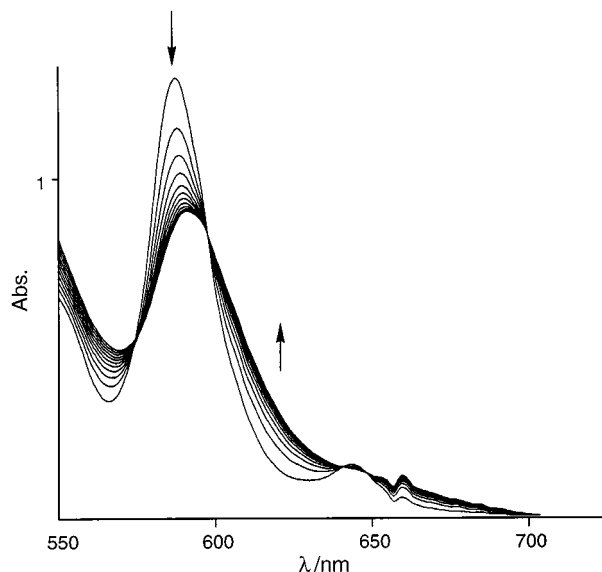
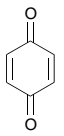
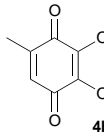
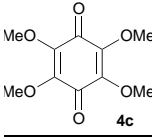


Fig. 3 UV–VIS spectral change of **1** on addition of ubiquinone (**4h**) in CHCl₃ at 298 K.

thermodynamic parameters are summarized in Table 1. The binding affinity of **1** for *p*-benzoquinone (**4a**) is similar to that of **2**. The latter has two hydroxy groups as an interaction site, suggesting that the two quinone carbonyl oxygens interact with the two hydroxy groups of 2-naphthol in **1** or **2**. Furthermore, in the case of 2,3-dimethoxy-5-methyl-*p*-benzoquinone (**4b**) and **4c**, the affinity of **1** for the quinone guest increases with the number of methoxy substituents on the quinone ring, whereas the presence of those methoxy groups has no effect on the interaction with **2**. According to the thermodynamic parameters obtained from variable-temperature experiments, a large enthalpic gain is observed upon formation of the **1·4b** and **1·4c** complexes as compared to formation of the **2·4b** or **2·4c** complexes, although there is no marked change in the entropic

Table 1 Binding constants (K_a) and thermodynamic parameters (ΔG° , ΔH° , $T\Delta S^\circ$) on complexation between porphyrin and quinone at 298 K^a

Host	1 (4 points) ^{b,c}	2 (2 points) ^{d,e}
	$K_a = 3.0 \times 10^3 \text{ M}^{-1}$ $\Delta G^\circ = -2.0 \text{ kcal mol}^{-1}$ $\Delta H^\circ = -6.5 \text{ kcal mol}^{-1}$ $T\Delta S^\circ = -4.5 \text{ kcal mol}^{-1}$	$K_a = 5.5 \times 10^3 \text{ M}^{-1}$ $\Delta G^\circ = -2.4 \text{ kcal mol}^{-1}$ $\Delta H^\circ = -5.6 \text{ kcal mol}^{-1}$ $T\Delta S^\circ = -3.3 \text{ kcal mol}^{-1}$
	$K_a = 5.4 \times 10^2 \text{ M}^{-1}$ $\Delta G^\circ = -3.7 \text{ kcal mol}^{-1}$ $\Delta H^\circ = -7.2 \text{ kcal mol}^{-1}$ $T\Delta S^\circ = -3.5 \text{ kcal mol}^{-1}$	$K_a = 3.5 \times 10^3 \text{ M}^{-1}$ $\Delta G^\circ = -2.1 \text{ kcal mol}^{-1}$ $\Delta H^\circ = -6.0 \text{ kcal mol}^{-1}$ $T\Delta S^\circ = -4.0 \text{ kcal mol}^{-1}$
	$K_a = 2.0 \times 10^4 \text{ M}^{-1}$ $\Delta G^\circ = -5.8 \text{ kcal mol}^{-1}$ $\Delta H^\circ = -10.5 \text{ kcal mol}^{-1}$ $T\Delta S^\circ = -4.7 \text{ kcal mol}^{-1}$	$K_a = 7.8 \text{ M}^{-1}$ $\Delta G^\circ = -1.2 \text{ kcal mol}^{-1}$ $\Delta H^\circ = -4.3 \text{ kcal mol}^{-1}$ $T\Delta S^\circ = -3.1 \text{ kcal mol}^{-1}$

^a Precision is generally estimated to be $\pm 10\%$. ^b Measured by UV–VIS titration in CHCl₃. ^c Ref. 11(a). ^d Measured by ¹H NMR titration in CDCl₃. ^e Ref. 8.

term. These results indicate that methoxy groups also act as interaction sites for the four 2-naphthols of **1**. Fig. 4 illustrates the comparison of binding constants between **1** and several ubiquinone analogues having two methoxy groups. Compared to 2,5-dimethoxy-*p*-benzoquinone (**4e**) and 2,6-dimethoxy-*p*-benzoquinone (**4f**), 2,3-dimethoxy-*p*-benzoquinone (**4d**) shows a large enhancement of its binding constant with **1**. The host **1** also binds native ubiquinone (**4h**) with a binding constant of $1.6 \times 10^2 \text{ M}^{-1}$ ($\text{M} = \text{mol dm}^{-3}$) at 298 K in CHCl_3 , although the long isoprenoid chain seems to bring about some steric repulsion. Furthermore, in solid state, the hydroxy groups of all naphthol groups interact with all the oxygen atoms of **4c**, showing an O–O distance of 2.68–3.21 Å.^{11c} It is suggested that two adjacent methoxy substituents at the 2- and 3-positions on the quinone ring cooperatively act as the effective third and/or fourth interaction sites *via* bifurcated hydrogen bonding. Thus, porphyrin **1** having four naphthol groups as binding sites seems to be a suitable host molecule for ubiquinone analogues.

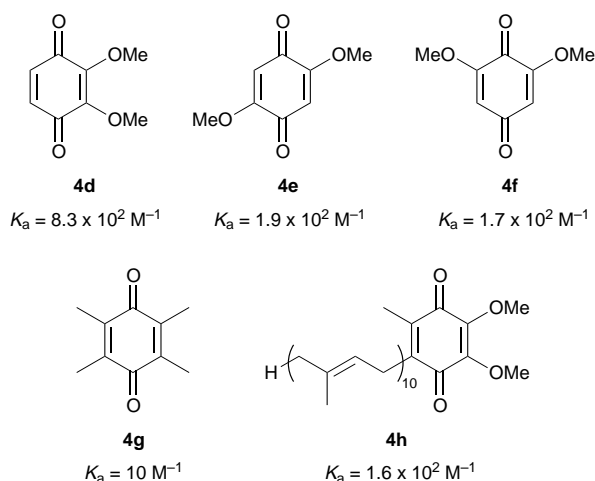


Fig. 4 Comparison of binding constants between **1** and dimethoxy-*p*-benzoquinones in CHCl_3 at 298 K

4.2 Photoinduced ET in porphyrin–quinone pairing *via* multi-hydrogen bonding

It is of particular interest to investigate the photoinduced ET by use of porphyrin–quinone assembly. The sufficient affinity of porphyrin **1** for ubiquinone analogues encouraged application of these complexes to the study of the ET reaction in this system. We used the zinc complex of **1** and *meso*- $\alpha,\alpha,\alpha,\alpha$ -tetra(7-hydroxy-1-naphthyl)porphyrin (**3**)^{13a} as probes of ET reaction (Fig. 5). From CPK molecular models the distances between the porphyrin plane and quinone of **1** and **3** are estimated to be 3.5 and 6.0 Å, respectively. Each zinc metallated porphyrin also has a good affinity for **4c** in toluene; $K_a(\mathbf{1Zn}\cdot\mathbf{4c}) = 2.5 \times 10^5 \text{ M}^{-1}$, $K_a(\mathbf{3Zn}\cdot\mathbf{4c}) = 2.2 \times 10^3 \text{ M}^{-1}$ at 298 K.

Dramatic changes in the fluorescence spectra of **1Zn** and **3Zn** have been observed upon addition of quinone and the Stern–Volmer plots indicate efficient fluorescence quenching of **1Zn** and **3Zn** in the low concentration range of quinone ($[\mathbf{4c}]_0 < 5 \times 10^{-3} \text{ M}$) as shown in Fig. 6. The findings demonstrate that static quenching of fluorescence occurs through ET from the photoexcited state of **1Zn** to **4c** in the cofacial mode. In contrast, no fluorescence quenching of zinc(II) *meso*- $\alpha,\alpha,\alpha,\alpha$ -tetra(2-methoxy-1-naphthyl)porphyrin (**5Zn**) was detected in the same concentration range as **4c**.

The time-resolved fluorescence measurements of **1Zn** and **3Zn** in toluene reveal monoexponential decay with a lifetime of 2.0 ± 0.1 and 2.2 ± 0.1 ns, respectively. The transient absorption spectra of **1Zn** or **3Zn** excited by dye laser pulse (570 nm, FWHM ≤ 3 ps) display a broad excited state absorption in the 615–750 nm region, which is assigned to a zinc porphyrin

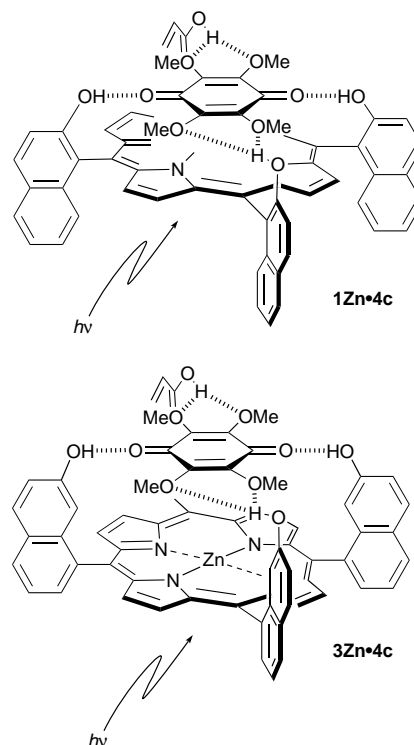


Fig. 5 Schematic complexation of **1Zn·4c** and **3Zn·4c** as an ET model system

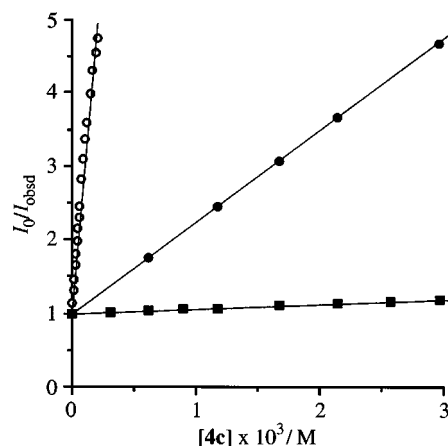


Fig. 6 Stern–Volmer plots for the fluorescence quenching of porphyrin **1Zn** (○), **3Zn** (●), and **5Zn** (■) with quinone **4c** in toluene at 293 K: excitation at 538, 541 and 540 nm for **1Zn**, **3Zn** and **5Zn**, respectively; emission at 645, 644 and 645 nm for **1Zn**, **3Zn** and **5Zn**, respectively; $[\mathbf{1Zn}] = 7.42 \times 10^{-5} \text{ M}$, $[\mathbf{3Zn}] = 7.36 \times 10^{-5} \text{ M}$, $[\mathbf{5Zn}] = 7.20 \times 10^{-5} \text{ M}$

singlet excited state. There was no substantial change in the spectra recorded within 50 ps delays after excitation by a laser pulse, which is consistent with the lifetime of the fluorescence. Upon addition of **4c** to **1Zn** and **3Zn** solutions, the transient absorption spectra show a significant time-dependent positive absorption at 640 nm as shown in Fig. 7. The spectra are characteristic of zinc porphyrin cation radical. The decays of the radical species as an intermediate of ET were fitted to monoexponential curves, which leads to the charge recombination constants of $(1.1 \pm 0.4) \times 10^{11} \text{ s}^{-1}$ for **1Zn·4c** and $(6.8 \pm 0.3) \times 10^{10} \text{ s}^{-1}$ for **3Zn·4c**. In contrast, forward ET rate constants were estimated to be $\geq 4 \times 10^{11} \text{ s}^{-1}$ (limited by the pulse width and signal-to-noise ratio) for both samples.^{13b}

Heitele, Michel-Beyerle, Staab and co-workers have reported the rate constants of charge separation and recombination in a series of covalently bridged porphyrin–quinone systems.¹⁴ For example, in the case of quinone-capped porphyrin **6**, the rate

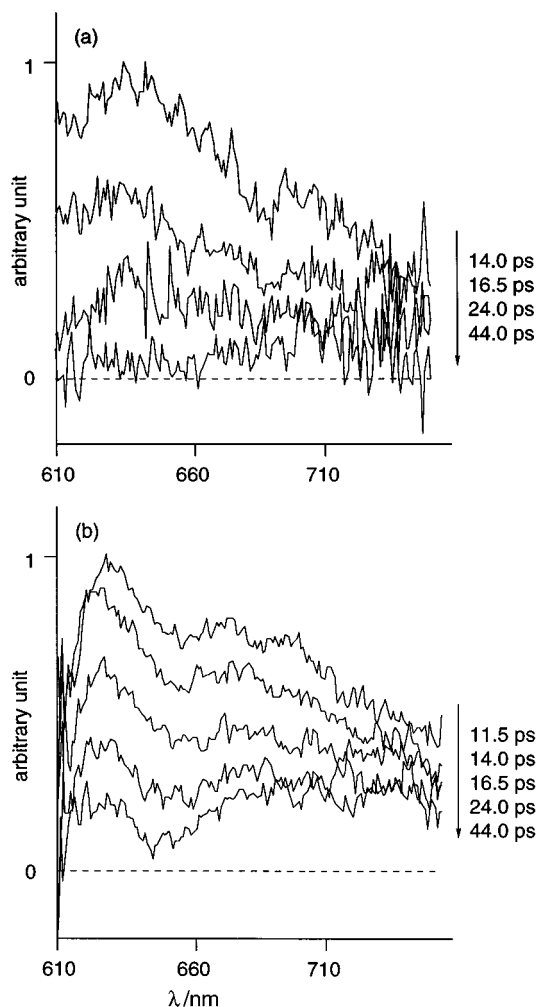
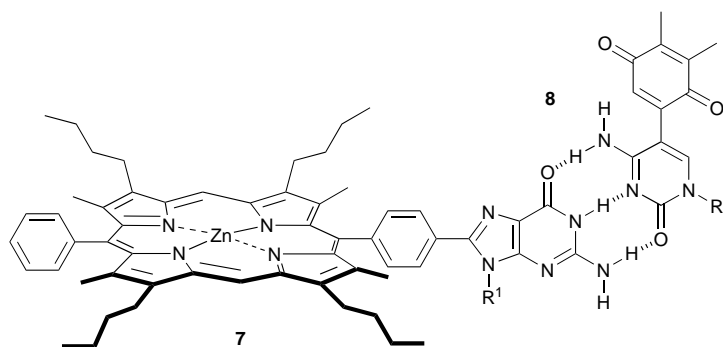
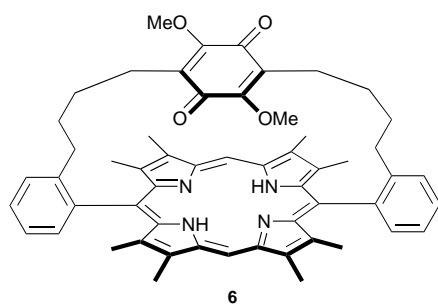


Fig. 7 Transient spectra after excitation at 570 nm (≤ 3 ps laser flash) in the presence of quinone **4c** (8.94×10^{-3} M) in toluene, showing the disappearance of the cation radical species. (a) **1Zn** (1.69×10^{-4} M); (b) **3Zn** (2.36×10^{-4} M)



constants corresponding to forward ET and charge recombination (backward) ET processes in toluene were determined to be 1×10^{11} and $3.9 \times 10^{10} \text{ s}^{-1}$, respectively. Although it is not easy to directly compare the ET rates between noncovalently and covalently linked porphyrin–quinone systems, the forward and thermal backward ET rate constants in our work are at least as large as those reported in Staab's compound.

Our present work demonstrates the first example of picosecond ET between zinc porphyrin and quinone linked in the cofacial mode by specific noncovalent interactions. It is noted that the ET rate is not limited by diffusion processes of donor nor acceptor and that the association by hydrogen bonding seems to be stable during the period of excitation, charge separation and recombination processes. Furthermore, one of the advantages of the present model is that we can easily examine many porphyrin–quinone pairings at the same time, since the host porphyrin binds various quinones *via* noncovalent interactions. Further investigation of the photochemistry of this system is in progress.

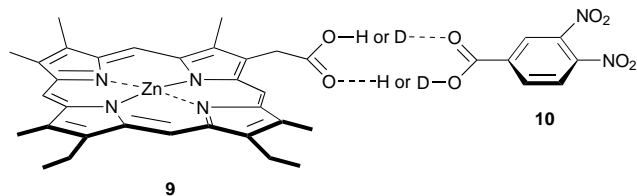
4.3 A sideways-linked porphyrin–quinone complex and its ET behaviour

Sessler and coworkers have recently presented another approach to design the noncovalently linked porphyrin–quinone ET system with an edge-to-edge separation distance of *ca.* 14 Å.^{9b} Porphyrin **7** and quinone **8** have guanosine and cytosine substituents, respectively, as recognition sites to form Watson–Crick hydrogen-bonding interaction. Upon addition of **8** to the CH_2Cl_2 solution of **7**, the quenching of zinc porphyrin fluorescence was observed and the fluorescence decay profile became biphasic with two exponential components of lifetimes $\tau_L = 1.8$ and $\tau_S = 0.74$ ns, respectively. Furthermore, the ratio of fraction amplitude of the two components leads to the binding constant of $(8.99 \pm 0.60) \times 10^3 \text{ M}^{-1}$, which is comparable with the estimated value from ^1H NMR titration. These results indicate that singlet ET from photoexcited **7** to **8** takes place with a rate constant of *ca.* $8 \times 10^8 \text{ s}^{-1}$ through exothermic process by 0.50 eV, although the porphyrin cation radical was not detected by picosecond laser flash photolysis. They have also prepared a well-organized energy-transfer system in noncovalently linked porphyrin–porphyrin complex by guanine–cytosine base pairing.¹⁵ The derived rate constants in both systems are not markedly dependent on the concentration of acceptors and the nature of interaction sites, indicating electron and/or energy transfer from donor to acceptor in the intra-aggregated complex formed by multipoint hydrogen bonding.

4.4 Mechanistic study on photoinduced ET in noncovalently linked donor–acceptor systems *via* hydrogen bonding

A slightly different approach to understanding the ET mechanism in noncovalently linked donor–acceptor systems has been taken by Nocera and co-workers. They have reported the intra-aggregated ET system of zinc porphyrin **9**–dinitrobenzoic acid **10** array mediated by hydrogen bonding.¹⁶ The binding constants for **9**–**10** and deuterated **9**–**10** pairs were estimated to

be 698 and 316 M⁻¹, respectively, by static fluorescence quenching. One of the interesting findings in this work is the isotropic effect on ET reaction from photoexcited **9** to **10**. The comparison of forward and charge recombination ET between protonated and deuterated carboxylic acid interfaces indicates the isotope effect of $k_H/k_D = 1.7$ and 1.6, respectively; rate constants of forward and charge recombination processes between **9** and deuterated **10** are 3.0×10^{10} and 6.2×10^9 s⁻¹, respectively. Their results indicate that the hydrogen bonding linkage between donor and acceptor may play a role in the ET process.



Therien and co-workers have recently presented significant ET model compounds in which zinc(II) porphyrin and iron(III) porphyrin are linked by hydrogen-, σ - and π -bonds, respectively.¹⁷ The singlet ET rate constants for three systems were determined by time-correlated single photon counting spectroscopy and the rate constant for hydrogen-bonding system **11** ($k_{ET} = 8.1 \times 10^9$ s⁻¹) is comparable to that for the π -bond system **12** ($k_{ET} = 8.8 \times 10^9$ s⁻¹), whereas the ET in system **13** composed totally of σ -symmetry bonds is slower ($k_{ET} = 4.3 \times 10^9$ s⁻¹) than that in **11** mediated by hydrogen bonds. The difference in the rate constants in these systems must derive from the magnitude of donor–acceptor electronic coupling, and they suggest that the electronic coupling modulated by a hydrogen-bond interface in **11** is greater than that provided by an interface composed of σ -bonds in **13**. The comparison of the ET reaction in their systems predicts that the hydrogen-bond interface in protein could mediate ET as efficiently as a covalent bridge.

5 Photoinduced ET in a protein complex by reconstituted zinc myoglobin

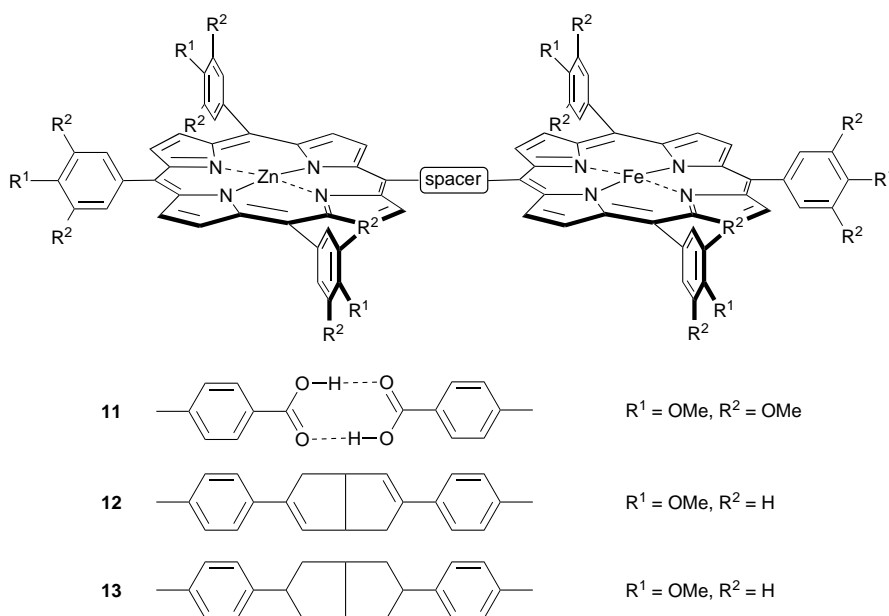
The next stage in the study of the respiratory system model is the construction of an artificial protein–electron carrier to investigate the role of molecular recognition and binding between electron donor and acceptor in biological ET systems. Over the past few years, elegant work focusing on mechanistic

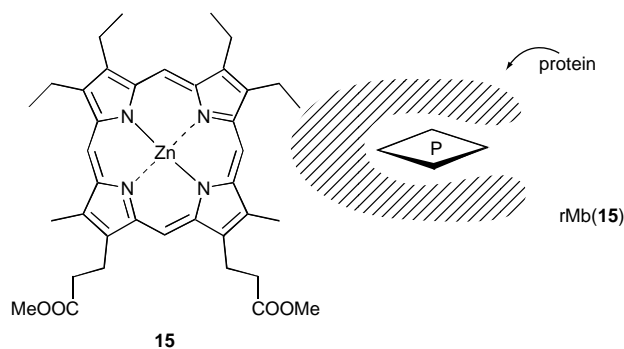
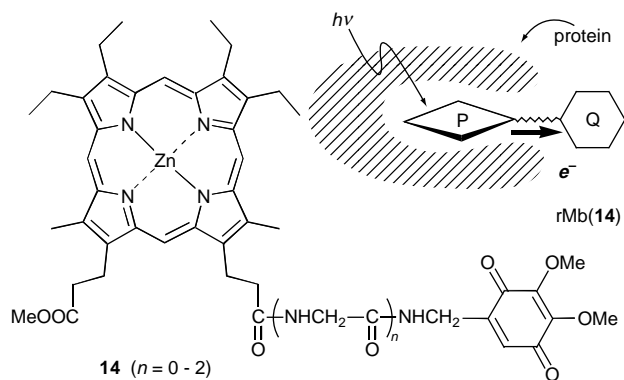
studies of the ET pathway in native and/or modified proteins have been reported by several groups.¹⁸ At the same time, a number of groups have also begun to focus on the intermolecular ET in a noncovalent protein–protein complex such as cytochrome c–cytochrome c peroxidase (CCP) pairing. Particularly, Hoffman^{18,19} McLendon,^{18,19} Millett¹⁹ and Kostić¹⁹ have demonstrated the relationship between interaction mode and ET rate in protein–protein complexes. To understand the ET mechanisms in self-associated protein–protein complexes, Rodgers has presented a mimetic system where a highly anionic uroporphyrin is bound to a positive cytochrome c *via* electrostatic docking forces.²⁰ These studies have suggested that the molecular recognition of redox proteins and their conformational interconversion upon binding seem to dominate not only the specificity of ET but also the ET rate. One major goal using a simple and efficient model is to understand how the ET is controlled by specific interface with the surface of protein. Thus it has been of particular interest to design artificial ET models based on modified proteins.

5.1 Photoinduced ET from zinc porphyrin to a linked quinone in protein

Myoglobin is one of the most popular haemoproteins as an oxygen-storage protein and it is well characterized in terms of both primary and tertiary structures, thereby facilitating model building. Unlike cytochrome c, the haem as a prosthetic group in myoglobin is not covalently bound to the protein core. This feature enables the replacement of native haem with an artificial metalloporphyrin, thus it facilitates the preparation of reconstituted myoglobin having a unique function. In the last decade, we have reported various myoglobins reconstituted with artificial haems and studied their properties, showing that some modification of the peripheral propionate at the 6- or 7-position of the haem structure induces no serious problem concerning protein stabilization.²¹ According to this result, we have prepared a new zinc porphyrin bearing a quinone component as an electron acceptor **14** (ZnP–Gly_n–Q, $n = 0$ –2) and incorporated **14** into apoprotein to obtain the reconstituted myoglobin rMb(**14**), which was characterized by TOF-mass, NMR, and UV–VIS spectroscopic measurements.²²

The photoinduced ET from zinc porphyrin to quinone in rMb(**14**) was monitored by fluorescence spectroscopy of the zinc porphyrin moiety in buffer solution (pH 7.0). As compared with the reference protein, rMb(**15**), the fluorescence intensity of rMb(**14**, $n = 2$) was weak and a shorter fluorescence lifetime of 0.6 ns was observed, whereas the fluorescence quenching of

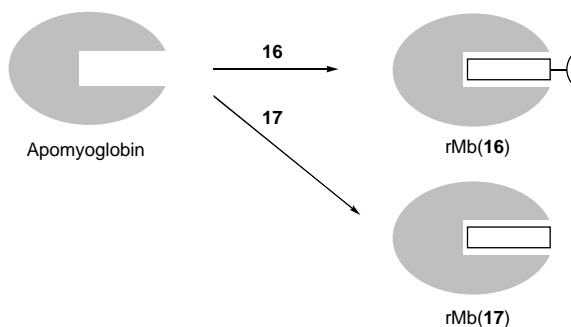
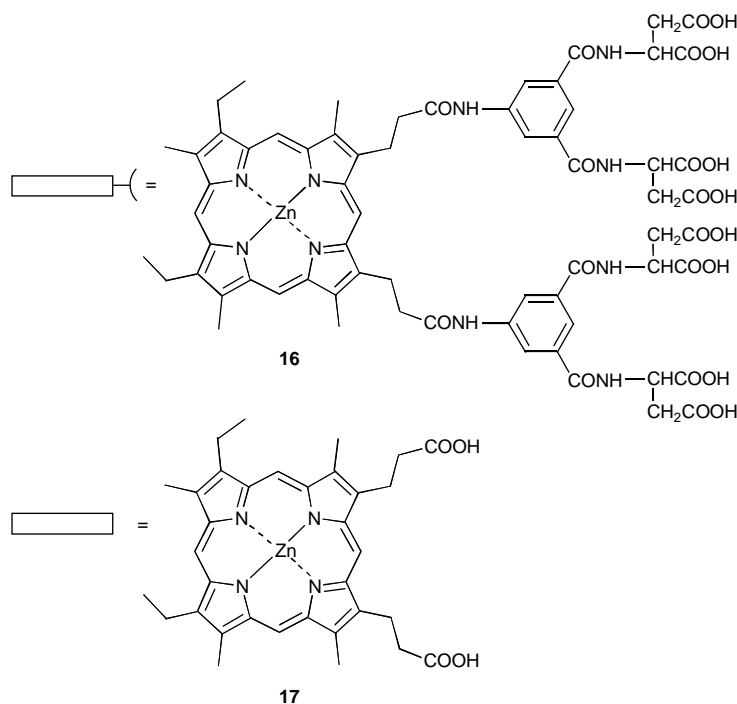




rMb(**15**) in the presence of quinone **4b** was not detected and the single exponential curve of fluorescence decay with $\tau = 1.9$ ns was observed. These results demonstrate that the singlet ET occurs from photoexcited zinc porphyrin to quinone in protein and the forward rate constant is estimated to be 1.1×10^9 s⁻¹ from the following equation: $k_{ET} = 1/\tau_1 - 1/\tau_2$, where τ_1 and τ_2 represent the fluorescence lifetime of rMb(**14**) and rMb(**15**). The result obtained indicates that the myoglobin reconstituted with synthetic zinc porphyrin is a suitable photodonor. Thus, we have taken a new approach to construct a noncovalently linked protein-acceptor model as shown in the following section.

5.2 Artificial recognition between reconstituted myoglobin and methyl viologen

According to the X-ray crystal structure analysis and a series of kinetic studies on cytochrome c receptors, it is found that the binding sites of cytochrome c on the surface of the receptor protein consist of several anionic residues forming special pairs with a few specific lysines of cytochrome c.⁶ On the basis of this concept, we have designed the novel zinc myoglobin rMb(**16**) having a negative recognition site for positively charged electron acceptors such as methyl viologen dication (**18**), as shown in Scheme 1.²³ Artificial prosthetic group, zinc porphyrin **16**, which has eight carboxylates at the terminal of 6- and 7-propionates of mesoporphyrin, was easily inserted into horse heart apomyoglobin by routine methodology. The stability of the myoglobin obtained rMb(**16**) was similar to that of the reference protein rMb(**17**) reconstituted with mesoporphyrin zinc complex **17**, and both characteristic visible absorption



Scheme 1

spectra and CD spectra were comparable. These features indicate that serious structural changes of the reconstituted protein do not result from the insertion of artificial porphyrin **16** into apomyoglobin.

A study of the fluorescence quenching of rMb(**16**) by **18** was monitored at 580 and 635 nm wavelengths in different solvent conditions. The Stern–Volmer plots in Fig. 8 show that there is static quenching in a low concentration of quencher **18** ($< 6 \times 10^{-3}$ M). Furthermore, efficient quenching is found at high pH and/or low ionic strength. In contrast, no fluorescence quenching of rMb(**17**) was observed upon addition of **18** ($< 10^{-2}$ M). These results indicate the ground-state complexation between rMb(**16**) and **18** via electrostatic recognition as shown in Scheme 2, in which donor and acceptor are separated by an edge-to-edge distance of 13–17 Å based on CPK models.

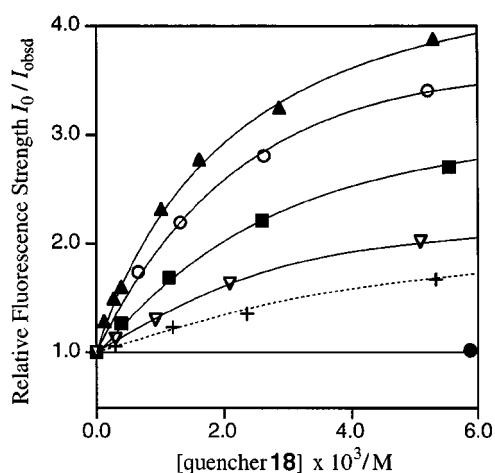
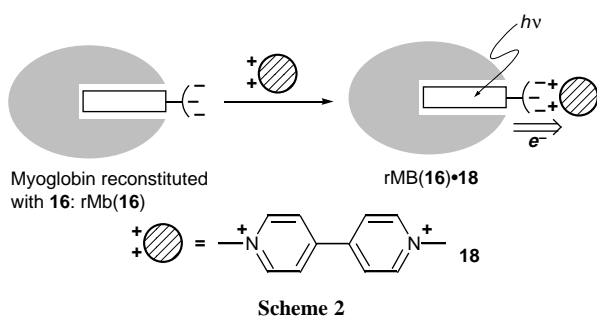


Fig. 8 Stern–Volmer plots for the fluorescence quenching of porphyrin rMb(**16**) and rMb(**17**) in the presence of **18** at various pH at 25 °C. The solid and dashed lines correspond to the data obtained in 10 and 100 mM phosphate buffers, respectively. rMb(**16**): pH = 5.76 (∇), pH = 6.10 (\blacksquare), pH = 6.41 (\circ), pH = 7.08 (\blacktriangle), pH = 7.00 ($+$). [rMb(**16**)] = 10^{-6} M. rMb(**17**): pH = 7.00 (\bullet). [rMb(**17**)] = 10^{-6} M. The changes of fluorescence emission were monitored at 584 nm ($\lambda_{\text{ex}} = 543$ nm).



5.3 Singlet ET between reconstituted myoglobin and methyl viologen

The measurement of fluorescence lifetime of rMb(**16**) and rMb(**17**) gave a monoexponential curve with a lifetime of 2.0 ± 0.1 ns, whereas, in the presence of **18**, fluorescence decay of rMb(**16**) exhibits a biphasic curve expressed by two lifetimes as shown in Fig. 9; $\tau_L = 2.0 \pm 0.1$ and $\tau_S = 0.4 \pm 0.1$ ns, respectively. The longer and shorter lived components of the decay curve are assignable to free rMb(**16**) and the rMb(**16**)·**18** complex, respectively, and the relative contribution of the shorter one, τ_S , increases with increasing concentration of **18**, which also supports the stable complexation between rMb(**16**) and **18** during the ET process. From the lifetime results the rate constant of forward singlet ET (k_{et}^S) from photoexcited rMb(**16**) to **18** is $2.1 \times 10^9 \text{ s}^{-1}$ derived as $k_{\text{et}}^S = 1/\tau_S - 1/\tau_L$.

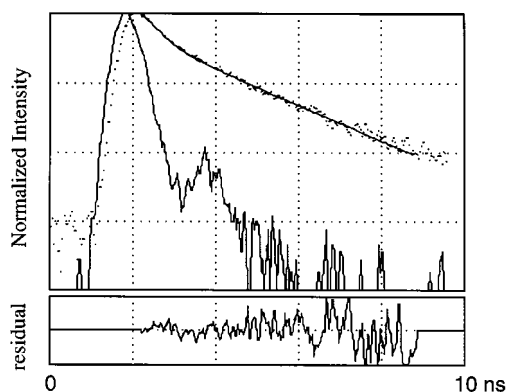


Fig. 9 Fluorescence decay profiles obtained from rMb(**16**) solution in the presence of **18** at room temperature in pH 7.0, 10 mM phosphate buffer with excitation wavelength at 543 nm. [rMb(**16**)] = 2.8×10^{-6} M and [**18**] = 1.4×10^{-2} M. $\tau_S = 0.4$ ns ($A_S = 0.76$), $\tau_L = 1.8$ ns ($A_L = 0.24$).

Transient absorption spectra of rMb(**16**) in the presence of **18** were monitored by a streak camera after a 50 ps, 532 nm laser flash. A strong absorption band centred at 455 nm can be assigned to the superposition of excited singlet and triplet states and cation radical species of zinc porphyrin in myoglobin. These data support direct evidence of ET from rMb(**16**) to **18** and can lead to the kinetic analysis of the intermediate species; the charge recombination of cation radical species was directly monitored with a rate constant of $k_{\text{cr}} = 3.3 \times 10^8 \text{ s}^{-1}$.²⁴

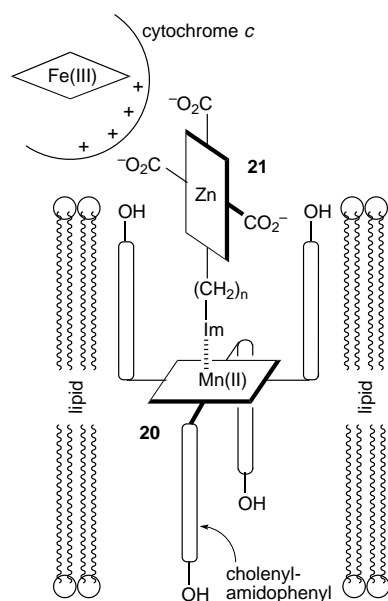
In contrast, the transient absorption spectra for rMb(**17**) in the presence of **18** show no clear decay of absorption in the same time range. According to the previous literature,²⁵ the photo-induced ET from triplet state of zinc myoglobin to **18** is diffusion controlled, whereas no such singlet ET reaction has been reported for zinc myoglobin. To our knowledge, the present work is the first example of a singlet ET between zinc myoglobin and electron acceptor *via* intermolecular interaction. Our results suggest that fast and/or efficient ET in biological systems is regulated by specific binding sites. At present, we are preparing a new myoglobin reconstituted with zinc porphyrin, having a different type of interface at the propionate terminus to compare the binding mode of **18** with rMb(**16**). Recent work shows that rMb(**16**) with eight carboxylate groups as an interface is one of the best receptors for **18**, thus, the degree of localization of anionic charges on the surface of protein should be quite important for the recognition of **18** in aqueous solution.²⁶

5.4 Future directions: protein–protein complexation

One of our aims is to construct artificial systems where reconstituted myoglobin interacts with redox protein such as cytochrome c in order to elucidate the recognition event at a molecular level. Upon the binding of methyl viologen with the present reconstituted myoglobin, the recognition behaviour should be attributable to point-to-point interaction by use of electrostatic forces. In contrast, it is expected that the essential feature of protein–protein complexation might depend on face-to-face recognition mode with multipoint interaction. Therefore, considering the design of an artificial protein–protein complex, it is necessary to note the distribution of special residues which play a binding-domain role with partner protein. Although clear evidence of the interaction between rMb(**16**) and cytochrome c has never been obtained by spectroscopic measurements, we have recently found a new myoglobin rMb(**19**) which has sufficient affinity for cytochrome c.²⁷ Functional groups of **19**, which are designed to match the position of particular lysines in cytochrome c, are slightly different from those of **16**. We will report the novel protein–protein complex and its ET behaviour within the specific interaction in the near future. It is likely that the reconstituted myoglobins such as rMb(**16**) or rMb(**19**) are good probes to

investigate the binding sites of partner protein and gating mechanism in ET processes.^{18,19}

Another recent model of ET in nature is the construction of multicomponent systems in artificial bilayers to mimic the mitochondrial membrane. Recently, Groves and co-workers have reported an elegant model where electron moves from the membrane spanning Mn^{II} porphyrin to cytochrome c *via* trianionic zinc porphyrin which is located on the surface of the membrane and designed to match the binding site of cytochrome c.²⁸ Spectral titrations of the cytochrome c to the **20–21** vesicular complex show the formation of a 1 : 1 adduct with a binding constant of $5 \times 10^6 \text{ M}^{-1}$. Electron transfer rate from Mn^{II} porphyrin in the **20**-DPPC/DMPC vesicle to cytochrome c was found to be first order and independent of the length of the imidazole tail of **21** with a rate constant of 10^3 s^{-1} , however, the rate obtained in the shorter DLPC lipid was ten times faster than that observed in DPPC/DMPC vesicles. These results support the stable **20–21**–cytochrome c ternary complexation and electron transfer *via* multiple pathway in the membrane ensembles. This research is one of the new approaches to the construction of nanoscale charge-separation systems to elucidate the ET mechanism of cytochrome c as a positive-charge membrane protein.



Lipid = dipalmitoylphosphatidylcholine (DPPC) and dimyristoylphosphatidylcholine (DMPC) or dilaurylphosphatidylcholine (DLPC)

6 Conclusion

It is well-known that molecular recognition processes are important in biological systems, such as enzymatic reactions, transportation, regulation *etc.*, as protein interfaces are frequently composed of intermolecular salts bridges, hydrogen bonds as well as extensive hydrophobic surface contacts. ET is also controlled by molecular recognition between the oxidoreductase and the electron carrier, which gives rise to efficient binding in the respiratory systems, although the mechanism is not clear. This has stimulated a variety of studies, especially on intermolecular ET process by use of noncovalently linked donor–acceptor models. In this review, we indicated new approaches to systems based on noncovalently linked donor–acceptor pairs as an ET model, focused on the molecular recognition of electron carriers; one is the specific receptor for quinones by multifunctional porphyrin and another is the reconstituted zinc myoglobins having the anionic interface for viologen dication and cytochrome c. It is reasonable to think that both of them could be widely useful for the elucidation of ET mechanisms, thanks to the following advantages: (i) they

link recognition behaviour with ET process and (ii) it is possible to monitor the stable charge-separation species in each model by spectroscopic measurements. The methodology of the construction of the noncovalently linked donor–acceptor pairs as simple models might provide a new insight into the complicated biological ET process.

7 Acknowledgements

We thank our collaborators, Professor Keitaro Yoshihara and Dr Shigeichi Kumazaki at the Institute for Molecular Science, and Professor Hideki Masuda at Nagoya Institute of Technology. We are deeply indebted to our colleagues for their excellent experiments. In particular, we appreciate the significant contributions made by several graduate students, Tetsuo Takimura, Takashi Miyahara, Tomohito Asai and Yutaka Hitomi.

8 References

- J. Deisenhofer, O. Epp, K. Miki, R. Huber and H. Michel, *Nature*, 1985, **318**, 618.
- M. R. Wasielewski, *Chem. Rev.*, 1992, **92**, 435.
- H. Kurreck and M. Huber, *Angew. Chem., Int. Ed. Engl.*, 1995, **34**, 849.
- J. L. Sessler, B. Wang, S. L. Springs and C. T. Brown, in *Comprehensive Supramolecular Chemistry*, Vol. 4, ed. Y. Murakami, Pergamon, Oxford, 1996, p. 311.
- K. Sakamoto, H. Miyoshi, K. Takegami, T. Mogi, Y. Anraku and H. Iwamura, *J. Biol. Chem.*, 1996, **271**, 29897.
- H. Pelletier and J. Kraut, *Science*, 1992, **258**, 1748.
- T. Tsukihara, H. Aoyama, E. Yamashita, T. Tomizaki, H. Yamaguchi, K. Shinzawa-Itoh, R. Nakashima, R. Yaono and S. Yoshikawa, *Science*, 1995, **269**, 1069; S. Iwata, C. Ostermeier, B. Ludwig and H. Michel, *Nature*, 1995, **376**, 660.
- Y. Aoyama, M. Asakawa, Y. Matsui and H. Ogoshi, *J. Am. Chem. Soc.*, 1991, **113**, 6233.
- (a) A. Harriman, Y. Kubo and J. L. Sessler, *J. Am. Chem. Soc.*, 1992, **114**, 388; (b) J. L. Sessler, B. Wang and A. Harriman, *J. Am. Chem. Soc.*, 1993, **115**, 10418; (c) A. Berman, E. S. Izraeli, H. Levanon and B. Wang, *J. Am. Chem. Soc.*, 1995, **117**, 8252.
- Other models of non-covalently linked porphyrin–quinone systems: M. Gonzalez, A. McIntosh, J. Bolton and A. Weedon, *J. Chem. Soc., Chem. Commun.*, 1984, 1138; Y. Kuroda, M. Ito, T. Sera and H. Ogoshi, *J. Am. Chem. Soc.*, 1993, **115**, 7003; H. Imahori, E. Yoshizawa, K. Yamada, K. Hagiwara, T. Okada and Y. Sakata, *J. Chem. Soc., Chem. Commun.*, 1995, 1133; F. D'Souza, *J. Am. Chem. Soc.*, 1996, **118**, 923; C. A. Hunter and R. J. Shannon, *Chem. Commun.*, 1996, 1361.
- (a) T. Hayashi, T. Miyahara, N. Hashizume and H. Ogoshi, *J. Am. Chem. Soc.*, 1993, **115**, 2049; (b) T. Hayashi, T. Miyahara, Y. Aoyama, M. Kobayashi and H. Ogoshi, *Pure Appl. Chem.*, 1994, **66**, 797; (c) T. Hayashi, T. Miyahara, N. Koide, Y. Kato, H. Masuda and H. Ogoshi, *J. Am. Chem. Soc.*, 1997, **119**, 7281.
- H. Ogoshi, Y. Kuroda, T. Mizutani and T. Hayashi, *Pure Appl. Chem.*, 1996, **68**, 1411.
- (a) T. Hayashi, T. Miyahara, Y. Aoyama, M. Nonoguchi and H. Ogoshi, *Chem. Lett.*, 1994, 1749; (b) T. Hayashi, T. Miyahara, S. Kumazaki, H. Ogoshi and K. Yoshihara, *Angew. Chem. Int. Ed. Engl.*, 1996, **35**, 1964.
- H. Heitele, F. Pöllinger, T. Häberle, M. E. Michel-Beyerle and H. A. Staab, *J. Phys. Chem.*, 1984, **98**, 7402; H. A. Staab, J. Weiser and E. Baumann, *Chem. Ber.*, 1992, **125**, 2275.
- A. Harriman, D. Magda and J. L. Sessler, *J. Phys. Chem.*, 1991, **95**, 1530.
- C. Turró, C. K. Chang, G. E. Leroi, R. I. Cukier and D. G. Nocera, *J. Am. Chem. Soc.*, 1992, **114**, 4013.
- P. J. F. deRege, S. A. Williams and M. J. Therien, *Science*, 1995, **269**, 1409.
- P. Bertrand, B. E. Bowler, J. Chang, B. M. Hoffman, H. B. Gray, A. Kuki, A. G. Mauk, G. McLendon, M. J. Natan, J. M. Nocek, A. L. Raphael, A. G. Sykes, M. J. Therien and S. A. Wallin, *Structure and Bonding*, vol. 25, Springer-Verlag, Berlin, 1991.
- G. McLendon and R. Hake, *Chem. Rev.*, 1992, **92**, 481; J. M. Nocek, J. S. Zhou, S. D. Forest, S. Priyadarshy, D. N. Beratan, J. N. Onuchic and B. M. Hoffman, *Chem. Rev.*, 1996, **96**, 2459; M. M. Ivković-Jensen and N. M. Kostić, *Biochemistry*, 1996, **35**, 15095; K. Wang, H. Mei, L. Geren, M. A. Miller, A. Saunders, X. Wang, J. L. Waldner,

- G. J. Pielak, B. Durham and F. Millett, *Biochemistry*, 1996, **35**, 15107.
- 20 J. S. Zhou and M. A. J. Rodgers, *J. Am. Chem. Soc.*, 1991, **113**, 7728.
- 21 T. Hayashi, Y. Hitomi, A. Suzuki, T. Takimura and H. Ogoshi, *Chem. Lett.*, 1995, 911.
- 22 T. Hayashi, T. Takimura, Y. Hitomi, T. Ohara and H. Ogoshi, *J. Chem. Soc., Chem. Commun.*, 1995, 545; 2503.
- 23 T. Hayashi, T. Takimura and H. Ogoshi, *J. Am. Chem. Soc.*, 1995, **117**, 11606.
- 24 N. Mataga, A. Karen, T. Okada, S. Nishitani, N. Kurata, Y. Sakata and S. Misumi, *J. Phys. Chem.*, 1984, **88**, 5138.
- 25 Recent review on ET in zinc myoglobin and methyl viologen **18**: K. Tsukahara, M. Okada, S. Asami, Y. Nishikawa, N. Sawai and T. Sakurai, *Coord. Chem. Rev.*, 1994, **132**, 223.
- 26 T. Hayashi, A. Tomokuni, T. Takimura and H. Ogoshi, unpublished results.
- 27 T. Hayashi, Y. Hitomi and H. Ogoshi, submitted for publication.
- 28 J. Lahiri, F. D. Fate, S. B. Ungashe and J. T. Groves, *J. Am. Chem. Soc.*, 1996, **118**, 2347.

Received, 28th January 1997

Accepted, 27th May 1997